European Journal of Taxonomy 1048: 142–163
https://doi.org/10.5852/ejt.2026.1048.3239

europeanjournaloftaxonomy.eu
ISSN 2118-9773
2026 · Ghosh A. *et al.*

Received: 30 September 2025 • *Accepted: 9 February 2026* • *Published: 2 April 2026*

Topic editor: Peter Vďačný • *Section editor: Tony Robillard* • *Desk editor: Eva-Maria Levermann*

Research article

urn:lsid:zoobank.org:pub:46C965B0-9A82-4EC9-901C-D9F733325315

Unveiling soil ciliate diversity: Taxonomy of two novel hypotrich ciliates (Alveolata: Ciliophora) from agricultural soil in Mathura, India

Arnab GHOSH[1], Daizy BHARTI[2], Antonietta LA TERZA[3], Rakesh BHUTIANI[4], Prakash Chand PATHANIA[5] & Santosh KUMAR[6,*]

[1,2,6]Zoological Survey of India, Prani Vigyan Bhawan, M-Block, New Alipore, Kolkata 700053, India.
[1]Department of Zoology, University of Calcutta, Kolkata 700073, West Bengal, India.
[3]School of Bioscience and Veterinary Medicine, University of Camerino, Via Gentile III da Varano, I-62032 Camerino (MC), Italy.
[4]Department of Zoology and Environmental Science, Gurukula Kangri (deemed to be University), Haridwar, India.
[5]High Altitude Regional Centre, Zoological Survey of India, Saproon 173211, Solan, Himachal Pradesh, India.

[*]Corresponding author: santoshkumar@zsi.gov.in, santoshcbio@gmail.com
[1]Email: write2aghosh@gmail.com
[2]Email: daizybharti83@gmail.com
[3]Email: antonietta.laterza@unicam.it
[4]Email: rbhutiani@gmail.com
[5]Email: pathaniapc@yahoo.co.in

Abstract. The present study investigates the morphology of two novel hypotrich ciliates, *Pseudourosomoida kadamberiae* gen. et sp. nov. and *Neoholosticha vikali* gen. et sp. nov., using live observation and protargol staining. These species were isolated from a soil sample collected from a pumpkin field in Mathura, India. *Pseudourosomoida kadamberiae* has an ellipsoid body (~58 × 21 µm in protargol preparations), two macronuclear nodules, no micronucleus, colorless to yellowish cortical granules, four dorsal kineties, an adoral zone composed of 17–30 membranelles, and no caudal cirri. Its morphogenesis begins with the development of an oral primordium near the leftmost transverse cirrus, similar to that in species of the genus *Urosomoida* Hemberger in Foissner, 1982. *Neoholosticha vikali* has a body size of ~115 × 31 µm in protargol preparations, yellowish-green cortical granules, ~85 ellipsoidal macronuclear nodules, one or two micronuclei, three frontal cirri, one buccal cirrus, two transverse cirri, about 45 cirri in the left and 48 in the right marginal rows, an adoral zone with ~32 membranelles, 6–8 dorsal kineties, and 7–12 caudal cirri. The study provides a detailed taxonomic account of both species, contributing to the understanding of soil ciliate diversity from India.

Keywords. *Holosticha*, morphology, *Neoholosticha vikali*, *Pseudourosomoida kadamberiae*, soil biodiversity.

Ghosh A., Bharti D., La Terza A., Bhutiani R., Pathania P.C. & Kumar S. 2026. Unveiling soil ciliate diversity: Taxonomy of two novel hypotrich ciliates (Alveolata: Ciliophora) from agricultural soil in Mathura, India. *European Journal of Taxonomy* 1048: 142–163. https://doi.org/10.5852/ejt.2026.1048.3239

Introduction

Soils harbor nearly 59% of the global terrestrial biodiversity (Anthony *et al.* 2023), yet protists, particularly ciliates, remain among the least explored and most functionally important components. Ciliated protists are key regulators of microbial populations, nutrient turnover, and soil fertility, with particularly critical roles in agroecosystems where biodiversity sustains ecosystem services and crop productivity. Yet, their diversity and distribution remain poorly characterized at both the taxonomic and ecological levels (Foissner 1987, 1992). Recent efforts, including a renewed focus on soil protistology (Geisen *et al.* 2017) and comparative analyses between natural and arable soils (Bharti *et al.* 2024), have begun to reveal how land use influences their community structure. However, a comprehensive understanding is still lacking, and only a limited number of studies have provided detailed species-level characterizations of agricultural soil ciliates (e.g., Bharti *et al.* 2015; Ghosh *et al.* 2024, 2025).

Rigorous taxonomic research, based on morphology and ontogenesis, is therefore essential, as it provides the foundation for ecological and biogeographic studies. As emphasized by Warren *et al.* (2017), advancing ciliate research equires the integration of ecological perspectives with robust taxonomic frameworks to fully understand their roles in soil ecosystems. In this study, we describe two novel hypotrich ciliates from an agroecosystem in Mathura, India, providing detailed morphological and ontogenetic analyses that expand current knowledge of soil ciliate diversity.

The non-oxytrichid dorsomarginalian ciliate genus *Urosomoida* Hemberger in Foissner, 1982 was initially established by Hemberger in Foissner (1982), with *U. agilis* Engelmann, 1862 as the type species. It is primarily characterized by a reduced number of pre-transverse ventral and/or transverse cirri and the absence of dorsal kinety 3 fragmentation (Berger 1999). The genus was comprehensively reviewed by Berger (1999) and later by Shao *et al.* (2012), who assigned 13 species to *Urosomoida*. Foissner (2016) later established two closely related genera: *Oxytrichella*, with *Oxytrichella mahadjacola* Foissner, 2016 as the type species, and *Lepidothrix*, with *Lepidothrix dorsiincisura* (Foissner, 1982) Foissner 2016 as the type species. Additionally, Foissner (2016) erected the family Urosomoididae and placed six genera within it, all sharing the characteristics of having fewer frontal-ventral-transverse cirri and the absence of dorsal kinety fragmentation. These genera include *Urosomoida*, *Erimophrya* Foissner *et al.*, 2002, *Hemiurosomoida* Singh & Kamra, 2015, *Lepidothrix*, *Oxytrichella*, and *Paraurosomoida* Singh & Kamra, 2013 (Foissner 1982, 2016; Hemberger 1985; Foissner *et al.* 2002; Singh & Kamra 2013, 2015). In addition to these known genera, we have identified a new species under a new genus, *Pseudourosomoida kadamberiae* gen. et sp. nov., based on the morphological and ontogenetic characteristics observed in specimens from the soil sample collected in Mathura, India. The new species exhibits a distinct morphological feature, i.e., the absence of caudal cirri.

The family Holostichidae Fauré-Fremiet, 1961 was established by Fauré-Fremiet (1961) and is primarily characterized by the presence of three frontal cirri and a midventral complex composed exclusively of cirral pairs (Berger 2006). The family previously included eight genera: *Afrothrix* Foissner, 1999, *Anteholosticha* Berger, 2003, *Caudiholosticha* Berger, 2003, *Diaxonella* Jankowski, 1979, *Holosticha* Wrześniowski, 1877, *Periholosticha* Hemberger, 1985, *Psammomitra* Borror, 1972, and *Pseudoamphisiella* Song, 1996 (see Berger 2006). Later, Li *et al.* (2017), on the basis of morphology, morphogenesis, and a phylogenetic analysis of *Caudiholosticha stueberi* (Foissner, 1987) Berger 2003, placed the species within the genus *Uroleptus* Ehrenberg, 1831, making *Caudiholosticha* Berger, 2003 a subgenus of *Uroleptus*. Presently, *Uroleptus* (*Caudiholosticha*) contains two species: *U.* (*C.*) *stueberi*

(Foissner, 1987) Li *et al.* 2017 and *U.* (*C.*) *antarctica* Park *et al.*, 2018. Apart from these, all other 16 species being formerly assigned to *Caudiholosticha* were transferred to six new genera raised by Li *et al.* (2017), based on available morphological and molecular data: *Acuholosticha* Li *et al.*, 2017, *Adumbratosticha* Li *et al.*, 2017, *Caudikeronopsis* Li *et al.*, 2017, *Extraholosticha* Li *et al.*, 2017, *Limnoholosticha* Li *et al.*, 2017, and *Multiholosticha* Li *et al.*, 2017. Although they did not classify these genera at the family level, we believe that all these genera should belong to the family Holostichidae Fauré-Fremiet, 1961, as their morphology shares the characteristics outlined by Berger (2006: 85). However, Li *et al.* (2017) expressed doubt regarding the placement of *Caudikeronopsis*, as they were unsure whether the genus belongs to Pseudokeronopsidae Borror & Wicklow, 1983. Until further data are available, we tentatively consider this genus within Holostichidae. Subsequently, Song *et al.* (2021) transferred *Limnoholosticha viridis* (Kahl, 1932) Li *et al.* 2017 to *Bourlandella* Song *et al.*, 2021 and established a new family, Bourlandellidae Song *et al.*, 2021, based on its morphology, ontogenesis, and molecular phylogeny. In addition to the previously described genera, we have identified a new species belonging to a new genus within the family Holostichidae. This new species, discovered from the same soil sample collected in Mathura, India, exhibits distinct morphological features, such as more than three dorsal kineties and multiple caudal cirri.

A detailed description of both species is provided based on the examination of specimens in vivo and after protargol preparation.

Material and methods

A soil sample (approximately 150 g) was collected from an agricultural field in a pumpkin plantation on the left bank of the Yamuna River, near Shergarh Khadar village in the Mathura district, about 35 km north of Mathura, Uttar Pradesh, India. The sampling site lies close to the bridge where Shergarh Road and Hodal-Hassanpur Road cross the Yamuna River (27°47′50″ N, 77°36′50″ E). The sample was collected during a field trip in April, 2022. Ciliates were made to excyst using the non-flooded Petri dish method (Foissner *et al.* 2002), and the raw culture was maintained at a temperature of 18 ± 2°C, with the green alga *Chlorogonium elongatum* as the food source (Ammermann *et al.* 1974) and sterilized, crushed wheat grains. Live cell observations and photomicrography were conducted using a stereo microscope (SZ2-ILST, Olympus) and a bright-field microscope (CX 43, Olympus) equipped with an attached camera. The cells were fixed using 100% alcohol. The protargol method described by Kamra & Sapra (1990) and Foissner (1991) was used to reveal the infraciliature. Silver Proteinate (Merck), kindly provided by the late Prof. Wilhelm Foissner, was used for impregnation. Counts and measurements of specimens from protargol preparations were conducted at a magnification of 1000×. In vivo measurements were performed at magnifications of 40–1000×. Illustrations of live specimens were based on free-hand sketches and photomicrographs, while those of impregnated cells were made with a drawing device. The taxonomic summary and terminology follow Berger (1999, 2006), Foissner (2016), and Wallengren (1900). Unfortunately, the culture was lost, and attempts to recover both species failed; thus, we could not perform a molecular analysis. The physicochemical parameters of the soil were analyzed as described by Chaurasia & Gupta (2014).

The type material is stored in the Protozoology Section of the Zoological Survey of India, Kolkata (NZSI).

Abbreviations for morphological terms

AM = adoral membranelles
AZM = adoral zone of membranelles
BC = buccal cirrus
CC = caudal cirrus

CG = cortical granules
DK = dorsal kinety
DM = dorsomarginal kinety
E = endoral
FC = frontal cirrus
FT = frontoventral cirrus
FV = food vacuoles
FVC = frontoventral cirri
LM = left marginal cirral row
LMA = left marginal anlage
MA = macronuclear nodules
MI = micronuclei
MP = midventral pair
OP = oral primordium
P = paroral
PF = pharyngeal fiber
POVC = postoral ventral cirri
PTVC = pretransverse cirrus
RM = right marginal cirral row
RMA = right marginal anlage
TC = transverse cirrus

Results

Taxonomy

Class Spirotrichea Bütschli, 1889
Subclass Hypotrichia Stein, 1859
Order Hypotrichida Jankowski, 1979
Family Urosomoididae Foissner, 2016

Genus ***Pseudourosomoida*** gen. nov.
urn:lsid:zoobank.org:act:A0BCAE68-1415-4C9B-8B45-E3C687EC1870

Type species

Pseudourosomoida kadamberiae gen. et sp. nov.

Diagnosis

Urosomoididae without caudal cirri.

Etymology

The genus-group name is a composite of the Greek word ‘pseudo’ (‘false’) and the generic name *Urosomoida*. Feminine gender.

Pseudourosomoida kadamberiae gen. et sp. nov.
urn:lsid:zoobank.org:act:AECA73BB-485D-460E-ACDF-162B451E9BB0
Figs 1–4; Table 1

Diagnosis

Body size in vivo about 75 × 30 µm. Outline elliptical. Nuclear apparatus consists of two macronuclear nodules, micronucleus absent. Cortical granules colorless to slightly yellowish, loosely spaced, about 0.5 µm in diameter. Invariably three frontals, one buccal, four frontoventral, three postoral ventral, one pretransverse, and four transverse cirri. Left marginal row on average composed of 16 cirri, right marginal row of 17 cirri. Adoral zone extends about 34% of body length, on average composed of about 23 membranelles. Four dorsal kineties, including one dorsomarginal row.

Etymology

The species is dedicated to Ms Kadamberi in recognition of her support and assistance during the sampling campaign in the agricultural fields of Mathura.

Type material

Holotype

INDIA • slide with morphostatic protargol-impregnated specimens (marked by a black ink circle on back of slide); Uttar Pradesh, near Shergarh Khadar village in Mathura district, left bank of Yamuna River; 27°47′50″ N, 77°36′50″ E; 2 Apr. 2022; Santosh Kumar leg.; NZSI, slide Pt 5974.

Paratypes

INDIA • 2 slides (containing many morphostatic protargol-impregnated specimens) with relevant cells marked by black ink circles on the back of slides; same data as for holotype; NZSI, slides Pt 5972, Pt 5973.

Type locality

Soil from an agricultural field with a pumpkin plantation on the left bank of the Yamuna River, near Shergarh Khadar village in the Mathura district (27°47′50″ N, 77°36′50″ E), Uttar Pradesh, India.

Description

Body size 55–75 × 25–35 µm in vivo, usually about 75 × 30 µm, based on in vivo measurements (n = 3) and morphometric data (Table 1), with 25% addition for preparation shrinkage (Foissner *et al.* 2002; Kumar & Foissner 2016; Kumar *et al.* 2016). Length:width ratio about 2.8:1 (Table 1). Outline elliptical to narrowly elliptical; dorsoventrally flattened (Figs 1A–B, E–J, 2A, D–F; Table 1). Nuclear apparatus located within central quarters of cell, slightly left of midline, composed of two macronuclear nodules; micronuclei absent (Figs 1E–F, H, 2A, D; Table 1). Macronuclear nodules ellipsoidal to elongate ellipsoidal, on average 13 × 5 µm in protargol preparations; contain many nucleoli 1–5 µm across. Cortex flexible, with cortical granules arranged in loose rows, colorless to slightly yellowish, about 0.5 µm across. Contractile vacuole located slightly above mid-body near left cell margin; collecting canals lacking (Figs 1B, 2A). Cytoplasm contains few crystals of varying shapes measuring approximately 3–7 µm in length, along with lipid droplets about 4 µm in diameter (Figs 1A, D, 2A–B). Food vacuoles in posterior body portion, up to 12 µm across in vivo, containing bacteria and flagellates. Movement rapid, with moderate gliding speed.

Cirral pattern resembles that of *Urosomoida*. Three slightly enlarged frontal cirri, cilia about 15 µm long in vivo. Frontoventral cirri arranged in V-shape; cirrus III/2 slightly above level of frontoventral cirrus IV/3 (although, due to alcohol fixation and slightly tilted orientation in permanent preparations,

it appears aligned in straight line). Buccal cirrus at level of anterior end of endoral, about 7 μm from anterior body end. Three postoral ventral cirri in typical pattern (Figs 1A–B, E–F, H, 2A, D; Table 1). One pretransverse ventral cirrus; four transverse cirri in oblique pseudorow, cilia about 18 μm long in

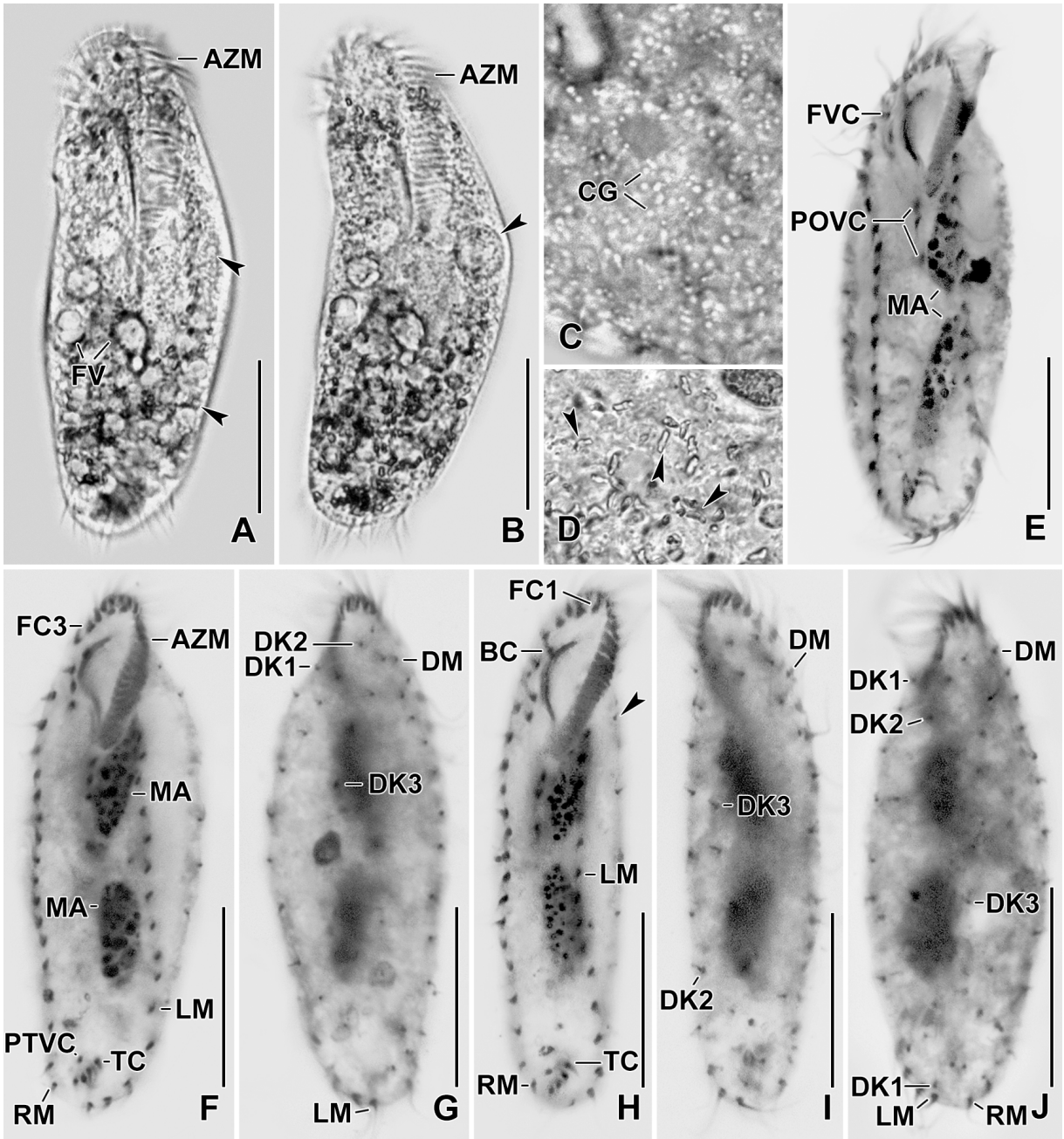

Fig. 1. *Pseudourosomoida kadamberiae* gen. et sp. nov., photomicrographs. **A–D**. Live specimens. **E–J**. Protargol-impregnated specimens. **A–B**. Ventral views of a slightly squeezed specimen showing lipid droplets (arrowheads in A) and the contractile vacuole (arrowhead in B). **C**. Cortical granules. **D**. Enlarged view of colorless crystals in the cytoplasm (arrowheads). **E, H–J**. Paratype specimens (NZSI) showing oral and somatic infraciliature and nuclear apparatus. **E, H**. Ventral views; arrowhead in H indicates dorsal kinety 1. **F–G**. Holotype (NZSI). **F**. Ventral view. **G**. Dorsal view. **I–J**. Dorsal views. Abbreviations: see Material and methods. Scale bars: A–B = 30 μm; E–J = 20 μm.

vivo, all cirri protruding beyond posterior cell end (Figs 1A–B, E–F, H, 2A, D; Table 1). Marginal cirral rows separate posteriorly, cirri about 10 µm long in vivo. Right row ends almost at, or slightly below (in most specimens), level of pretransverse cirrus; left row extends to body midline posteriorly. Left marginal row composed of an average of 16 cirri, right row of 17 cirri (Figs 1E–F, H, 2A, D; Table 1).

Constantly four (n = 21) dorsal kineties with bristles about 3 µm long in vivo and in protargol preparations. Kinety 1 slightly shortened anteriorly, composed of 9 bristles on average. Kineties 2 and 3 roughly bipolar, each composed of 12 bristles on average. Kinety 4 (= dorsomarginal row) slightly shortened posteriorly, composed of 13 bristles on average (Figs 1G, I–J, 2E–F; Table 1). Caudal cirri absent.

Adoral zone extends to about 34% of body length with approximate DE-value of 0.2 (for explanation, see Berger 2006), composed of an average of 23 membranelles with largest bases about 4 µm long in protargol preparations (Figs 1A–B, E–F, H, 2A, D; Table 1). Buccal cavity narrow and deep. Undulating membranes distinctly curved, optically intersecting at middle (Figs 1A–B, E–F, H, 2A, D). Paroral about 10 µm long, commencing about 5 µm posterior to anterior body end. Endoral about 10 µm long, commencing about 1 µm posterior to anterior end of paroral, at buccal cirrus level (Figs 1A–B, E–F, H, 2A, D; Table 1). Pharyngeal fibres extend slightly obliquely to right body margin (Figs 1F, H, 2A, D).

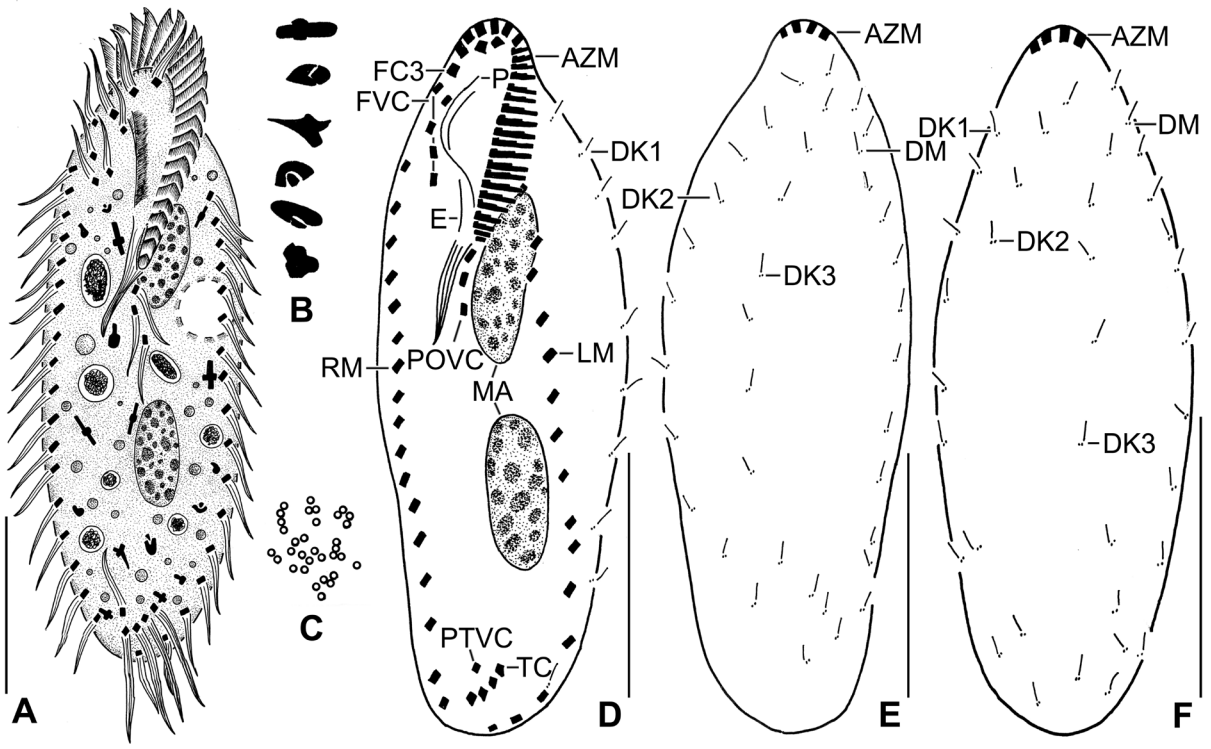

Fig. 2. *Pseudourosomoida kadamberiae* gen. et sp. nov., line diagrams. **A–C**. Live specimens. **D–F**. Protargol-impregnated specimens. **A**. Ventral view of a representative specimen. **B**. Enlarged view of cytoplasmic crystals. **C**. Cortical granules. **D–E**. Holotype (NZSI). **D**. Ventral view. **E**. Dorsal view. **F**. Paratype specimen (NZSI), dorsal view, showing infraciliature. Abbreviations: see Material and methods. Scale bars: A = 30 µm; D–F = 20 µm.

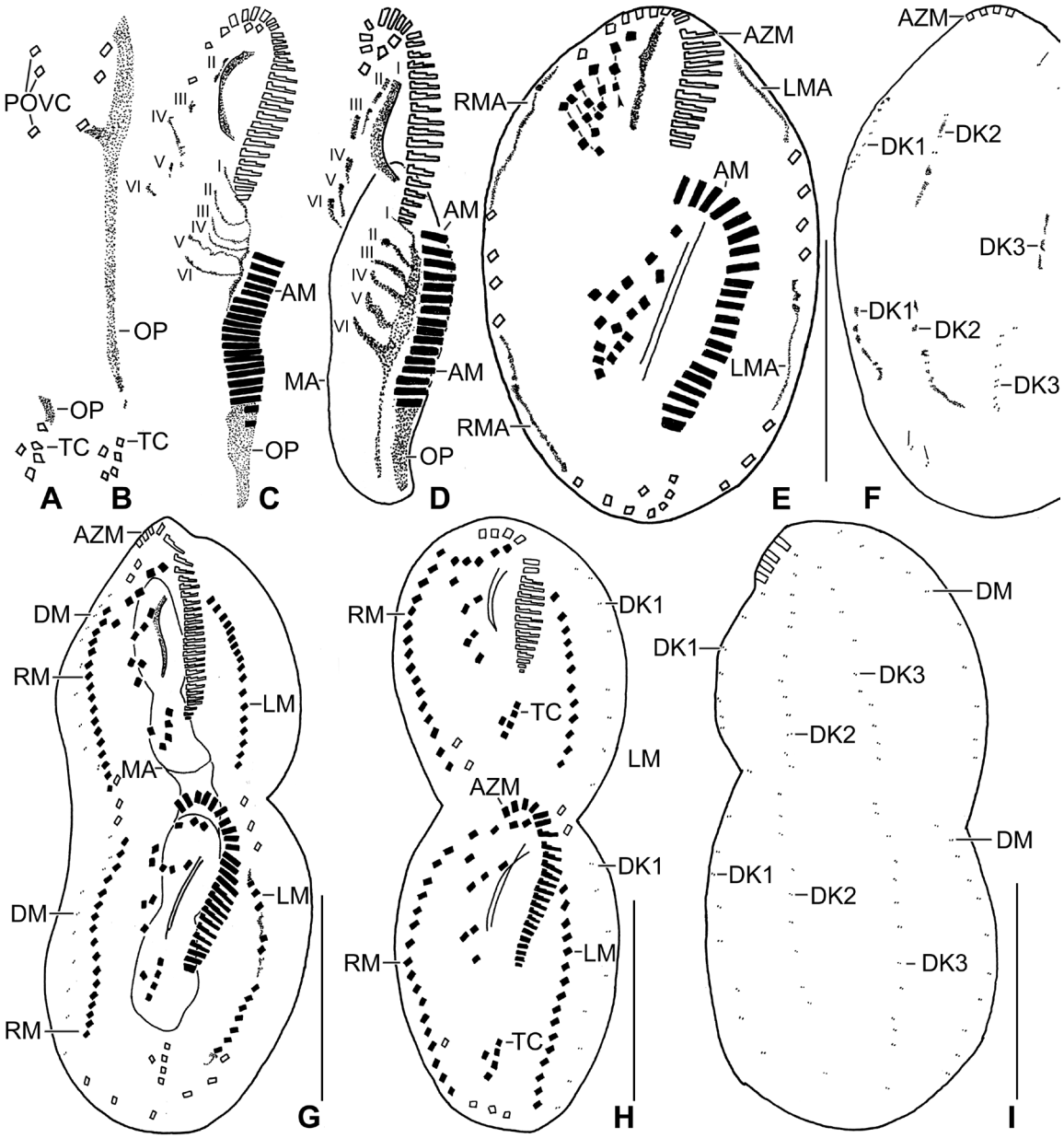

Fig. 3. *Pseudourosomoida kadamberiae* gen. et sp. nov., line diagrams of protargol-impregnated dividers (NZSI). **A–B, C, H–I**. Pt 5974. **D**. Pt 5972. **E–G**. Pt 5973. **A–B**. Oral primordium develops close to the leftmost transverse cirrus (A) and extends anteriorly (B). **C–D**. Six parental cirri (II/2, III/2, IV/2, IV/3, V/3, and V/4) disaggregate to give rise to frontal-ventral-transverse anlagen for both daughter cells; parental undulating membranes partially disintegrate to form anlage I; anlagen II–IV of the proter formed by disintegration of cirri II/2, III/2, and IV/3, respectively; anlagen V–VI of the proter possibly formed de novo; the postoral ventral cirri disaggregate and merge with the oral primordium to form anlagen I–VI for the opisthe. **E, G–I**. Six anlagen for both the proter and the opisthe segregate into a 1:2:3:3:3:4 cirral pattern (connected lines; arrowhead in E points to additional cirri that disintegrate later); the marginal anlagen arise at two levels by 'within-row' anlagen formation (E, G–H); dorsomarginal kineties originate close to the anterior end of newly formed right marginal cirral rows (G; see also Fig. 4D) and later shift dorsally (I). **F**. Specimen showing 'within-row' anlagen formation of dorsal kineties 1–3. Abbreviations: see Material and methods. Numerals denote cirral anlagen; numbering of cirri follows Wallengren (1900). Scale bars = 20 μm.

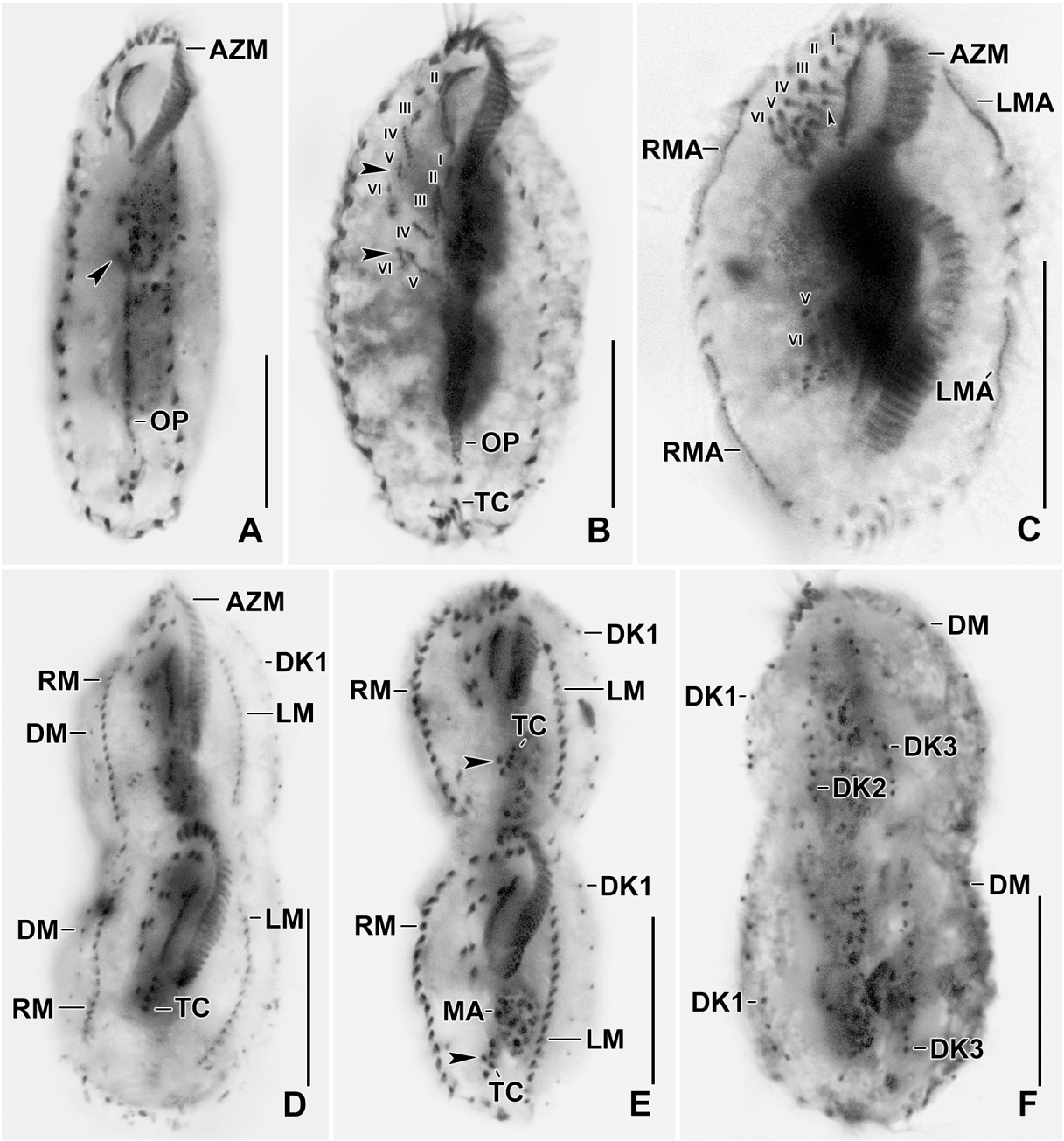

Fig. 4. *Pseudourosomoida kadamberiae* gen. et sp. nov., photomicrographs of protargol-impregnated dividers (NZSI). **A–B, E–F**. Pt 5974. **C–D**. Pt 5973. **A**. Oral primordium develops close to the leftmost transverse cirrus and extends anteriorly incorporating cirrus V/3 (arrowhead). **B**. Six parental cirri (II/2, III/2, IV/2, IV/3, V/3, and V/4) disaggregate to give rise to frontal-ventral-transverse anlagen for both daughter cells; arrowheads point to anlagen V and VI of the proter and opisthe, respectively. **C**. Mid-divider showing segregation of anlagen into a 1:2:3:3:3:4 cirral pattern; arrowhead indicates the additional cirrus that later disintegrates. **D–E**. Marginal anlagen arise at two levels by 'within-row' anlagen formation; dorsomarginal kineties originate close to the anterior end of newly formed right marginal cirral rows and later shift dorsally (D); arrowheads in E point to the pretransverse cirri. **F**. Specimen showing 'within-row' anlagen formation of dorsal kineties 1–3 and the newly formed dorsomarginal kinety. Abbreviations: see Material and methods. Numerals denote cirral anlagen; numbering of cirri follows Wallengren (1900). Scale bars = 20 μm.

Table 1 (continued in next page). Morphometric data on *Pseudourosomoida kadamberiae* gen. et sp. nov.

Characteristic[a]	Mean	M	SD	SE	CV	Min	Max	n
body, length	57.8	60.0	6.4	1.4	11.0	45.0	67.0	21
body, width	20.3	21.0	2.4	0.5	11.7	15.0	25.0	21
body length:width, ratio	2.8	2.8	0.4	0.1	14.0	2.1	3.6	21
body width:length, percentage	36.4	36.2	5.2	1.1	14.2	27.7	46.7	21
anterior body end to proximal end of adoral zone, distance	19.3	20.0	2.1	0.5	10.9	16.0	26.0	21
anterior body end to distal end of adoral zone, distance	3.3	3.0	0.6	0.1	17.3	2.0	4.0	21
anterior body end to proximal end of adoral zone, % of body length	33.6	33.3	3.7	0.8	11.1	27.6	43.3	21
anterior body end to distal end of adoral zone, % of body length	5.8	6.0	0.9	0.2	16.1	3.9	7.3	21
DE-value (see text)	0.2	0.2	0.0	0.0	18.4	0.1	0.2	21
adoral membranelles, width of longest base	3.6	4.0	0.7	0.1	18.5	3.0	5.0	21
adoral membranelles, number	23.0	23.0	2.6	0.6	11.1	17.0	30.0	21
widest gap between adoral zone of membranelles and paroral membrane	4.4	4.0	0.5	0.1	11.5	4.0	5.0	21
anterior body end to paroral membrane, distance	5.1	5.0	1.1	0.2	20.7	3.0	7.0	21
paroral membrane, length	10.2	10.0	1.5	0.3	15.1	8.0	14.0	21
anterior body end to endoral membrane, distance	5.9	6.0	1.1	0.2	19.2	4.0	9.0	21
endoral membrane, length	9.7	9.0	1.2	0.3	11.9	8.0	12.0	21
anterior body end to anterior macronuclear nodule, distance	14.5	15.0	2.3	0.5	15.6	10.0	19.0	21
posterior body end to posteriormost macronuclear nodule, distance	13.1	14.0	2.7	0.6	20.9	7.0	19.0	21
macronuclear figure, length	29.9	30.0	3.5	0.7	11.8	24.0	40.0	22
anteriormost macronuclear nodule, length	13.2	13.0	1.8	0.4	13.6	10.0	19.0	22
anteriormost macronuclear nodule, width	5.2	5.0	0.9	0.2	17.5	4.0	7.0	22
macronuclear nodules, number	2.0	2.0	0.0	0.0	0.0	2.0	2.0	21
anterior body end to right marginal row, distance	11.3	11	2.7	0.6	23.6	6.0	17.0	21
posterior body end to right marginal row, distance	2.1	2.0	0.8	0.2	39.7	1.0	4.0	21
right marginal row, number of cirri	17.2	17.0	1.7	0.4	9.9	12.0	21.0	21
anterior body end to left marginal row, distance	14.6	15.0	1.6	0.3	10.7	12.0	16.0	21
posterior body end to left marginal row, distance	1.1	1.0	0.4	0.1	31.4	1.0	2.0	21
left marginal row, number of cirri	16.0	16.0	1.4	0.3	8.9	14.0	20.0	21
gap between last cirri of marginal rows	3.6	4.0	0.9	0.2	25.9	2.0	5.0	21
frontal cirri, number	3.0	3.0	0.0	0.0	0.0	3.0	3.0	21
anterior body end to buccal cirrus, distance	6.8	7.0	1.3	0.3	18.7	4.0	9.0	21
buccal cirrus, number	1.0	1.0	0.0	0.0	0.0	1.0	1.0	21
anterior body end to posteriormost frontoventral cirrus, distance	13.0	13.0	2.0	0.4	15.2	8.0	16.0	21
frontoventral cirri, number	4.0	4.0	0.0	0.0	0.0	4.0	4.0	21
distance between buccal vertex and cirrus IV/2	1.6	1.5	0.6	0.1	39.0	1.0	3.0	20
distance between cirri V/3 and pretransverse cirrus	24.6	24.0	4.0	0.9	16.2	17.0	31.0	19
anterior body end to posteriormost postoral cirrus, distance	24.5	26.0	2.9	0.7	11.7	20.0	28.0	19
postoral cirri, number	3.0	3.0	0.0	0.0	0.0	3.0	3.0	19
posterior body end to pretransverse cirrus, distance	5.0	5.0	1.3	0.3	26.1	2.0	7.0	21
pretransverse cirri, number	1.0	1.0	0.0	0.0	0.0	1.0	1.0	21
posterior body end to leftmost transverse cirrus, distance	5.6	5.0	1.2	0.3	22.1	3.0	8.0	21
posterior body end to rearmost transverse cirrus, distance	2.7	3.0	0.9	0.2	35.2	1.0	5.0	21

Table 1 (continued).

Characteristic[a]	Mean	M	SD	SE	CV	Min	Max	n
transverse cirri, number	4.0	4.0	0.0	0.0	0.0	4.0	4.0	21
dorsal kineties, number	4.0	4.0	0.0	0.0	0.0	4.0	4.0	21
anterior body end to dorsal kinety 1, distance	9.0	9.0	1.3	0.3	14.2	7.0	11.0	21
dorsal kinety 1, number of bristles	9.5	9.0	1.2	0.3	12.6	8.0	13.0	18
anterior body end to dorsal kinety 2, distance	5.4	5.0	0.7	0.2	13.8	4.0	7.0	21
dorsal kinety 2, number of bristles	11.5	11.0	1.1	0.3	9.8	9.0	14.0	19
anterior body end to dorsal kinety 3, distance	5.1	5.0	1.2	0.3	24.4	3.0	8.0	20
dorsal kinety 3, number of bristles	11.6	12.0	1.4	0.3	12.0	9.0	14.0	18
dorsomarginal row, number of bristles	12.5	13.0	1.7	0.4	13.5	10.0	15.0	21
total dorsal bristles, number	45.2	45.0	2.64	0.6	5.9	41.0	50.0	18

[a] Data based on mounted, protargol-impregnated, and randomly selected specimens from a non-flooded Petri dish culture. Measurements in µm. Abbreviations: CV = coefficient of variation in %; M = median; Max = maximum; Mean = arithmetic mean; Min = minimum; n = number of individuals investigated; SD = standard deviation; SE = standard error of arithmetic mean.

Divisional ontogenesis

Ontogenesis begins with the de novo formation of basal bodies near the transverse cirrus III/1, gradually developing into an anarchic patch or oral primordium (OP) (Figs 3A–B, 4A). The anlage of the opisthe undulating membranes is generated by the proliferating kinetosomes extending towards the anterior right of the OP (Figs 3C–D, 4B). The undulating membranes anlage for the proter is formed by partial reorganisation of the parental undulating membranes. The parental adoral zone is retained for the proter, whereas the adoral zone of the opisthe is formed anew from the OP (Figs 3C–E, 4B–C).

The OP is extended by integrating postoral ventral cirri. The frontal-ventral-transverse cirral anlagen develop as follows. In the proter, parental undulating membranes partially disintegrate to form anlage I, which subsequently gives rise to the left frontal cirrus and the undulating membranes. Anlagen II–IV originate from the frontoventral cirri II/2, III/2, and IV/3, respectively. Anlagen V and VI are possibly formed de novo; further investigation is needed to determine their exact origin (Figs 3B–D, 4A–B). In the opisthe, six anlagen originate from the OP (Figs 3C–D, 4B). In total, six parental cirri (II/2, III/2, IV/2, IV/3, V/3, and V/4) and the parental undulating membranes contribute to the formation of six anlagen in both the proter and the opisthe (Figs 3A–D, 4A–B). The six anlagen divide in a 1:2:3:3:3:4 pattern, resulting in the formation of 16 frontal-ventral-transverse cirri (Figs 3E, G–H, 4C–E). The cirri V/2 (pretransverse cirrus) and II/1 (leftmost transverse cirrus) are absent.

The marginal anlagen arise at two levels by ‘within-row’ anlagen formation, utilizing one or two of the parental cirri at each level. The formation of the right marginal row begins earlier than that of the left row. The marginal primordia elongate, utilizing six to eight parental cirri, and differentiate into new marginal rows. The remaining parental marginal cirri are resorbed (Figs 3G, 4D).

On the dorsal surface, three anlagen are formed within dorsal kineties 1–3 at two levels (one set each for the proter and the opisthe). The kinety 3 anlage does not fragment. A dorsomarginal row arises close to the anterior end of the newly formed right marginal row and moves from the lateral to the dorsal surface in late dividers (Figs 3F–I, 4D–F). No caudal cirri are formed during cell division.

During nuclear division, the macronuclear nodules first fuse to form a single mass in middle dividers, and then divide twice to produce the typical four nodules in late dividers (Figs 3D, G, 4C–D).

Occurrence and ecology

Thus far, the species has been found only at the type locality. It feeds on bacteria and small flagellates. Other ciliates identified from the same soil sample include *Monomacrocaryon* sp., *Sterkiella tricirrata* (Buitkamp, 1977) Berger 1999, and *Sterkiella tetracirrata* Kumar *et al.*, 2014. The soil from which the species was isolated contained 0.72% moisture, and has a pH of 6.69, an electrical conductivity of 445 µS, a Na^+ concentration of 30.5 mg/l, a K^+ concentration of 49.1 mg/l, 1.56% organic carbon, and 2.68% organic matter.

Class Spirotrichea Bütschli, 1889
Subclass Hypotrichia Stein, 1859
Order Hypotrichida Jankowski, 1979
Superfamily Urostyloidea Bütschli, 1889
Family Holostichidae Fauré-Fremiet, 1961

Genus ***Neoholosticha*** gen. nov.
urn:lsid:zoobank.org:act:CBED5600-CDC6-4757-92E6-9453F0EFF1BA

Type species

Neoholosticha vikali gen. et sp. nov.

Diagnosis

Holostichidae with a continuous adoral zone of membranelles, frontoterminal cirri present, transverse cirri fewer than the midventral cirral pairs, more than four dorsal kineties, and multiple caudal cirri present.

Etymology

The genus-group name is a composite of the Greek prefix 'neo-' (meaning 'new') and the generic name *Holosticha*, referring to the similar frontoventral ciliature of *Holosticha* and *Neoholosticha*. Feminine gender.

Neoholosticha vikali gen. et sp. nov.
urn:lsid:zoobank.org:act:47ABAB9F-0A6B-4687-B605-428E74E7CB88
Figs 5–6; Table 2

Diagnosis

Size about 114 × 31 µm in protargol preparations. Body slender, narrowly elliptical. Cortical granules yellowish-green. Nuclear apparatus consists of 70–108 ellipsoidal macronuclear nodules scattered across the body and one or two micronuclei. Usually three slightly enlarged frontal cirri, one buccal cirrus, 2–4 frontoterminal cirri, 15–18 midventral pairs, and two ordinary-sized, vertically arranged transverse cirri. Left marginal row on average composed of 45 cirri, right row of 48 cirri. Adoral zone of membranelles extends about 27% of body length, on average composed of 32 membranelles. Undulating membranes arranged in the *Oxytricha* pattern. Dorsal ciliature consists of 6–8 dorsal kineties and 7–12 caudal cirri.

Etymology

The species is named after Mr Surender Vikal, a farmer in the sampling area, in recognition of his support and assistance during the sampling campaign in the agricultural fields of Mathura.

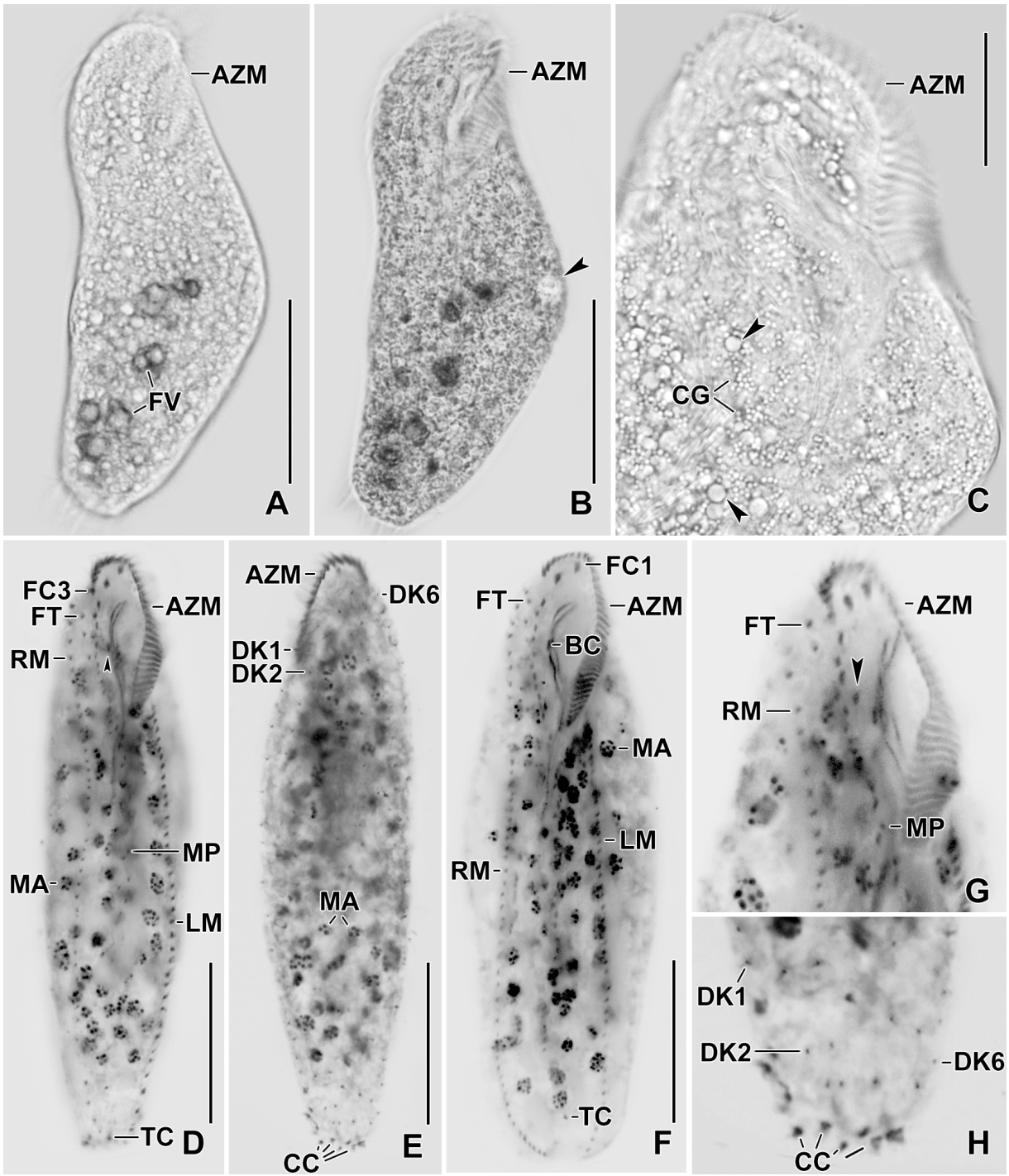

Fig. 5. *Neoholosticha vikali* gen. et sp. nov., photomicrographs. **A–C**. Live specimens. **D–H**. Protargol-impregnated paratype specimens. **A–B**. Ventral views of a squeezed specimen; arrowhead in B points to the contractile vacuole. **C**. Cortical granules; arrowheads denote lipid droplets. **D–E**. Ventral (D) and dorsal (E) views of holotype (NZSI) showing its infraciliature (see also Fig. 6C–D); arrowhead in D indicates the buccal cirrus. **F–H**. Ventral (F–G) and dorsal (H) views of paratype specimens (NZSI) depicting oral and somatic infraciliature and the nuclear apparatus; arrowhead in G indicates the parabuccal cirrus. Abbreviations: see Material and methods. Scale bars: A–B = 50 μm; C = 15 μm; D–F = 30 μm.

Type material

Holotype

INDIA • slide with morphostatic protargol-impregnated specimens (marked by a black ink circle on back of slide); Uttar Pradesh, near Shergarh Khadar village in Mathura district, left bank of Yamuna River; 27°47′50″ N, 77°36′50″ E; 2 Apr. 2022; Santosh Kumar leg.; NZSI, slide Pt 5974.

Paratypes

INDIA • 2 slides (containing many morphostatic protargol-impregnated specimens) with relevant cells marked by black ink circles on the back of slides; same data as for holotype; NZSI, slides Pt 5972, Pt 5973.

Type locality

Soil from an agricultural field in a pumpkin plantation on the left bank of the Yamuna River near Shergarh Khadar village in the Mathura district, Uttar Pradesh, India (27°47′50″ N, 77°36′50″ E).

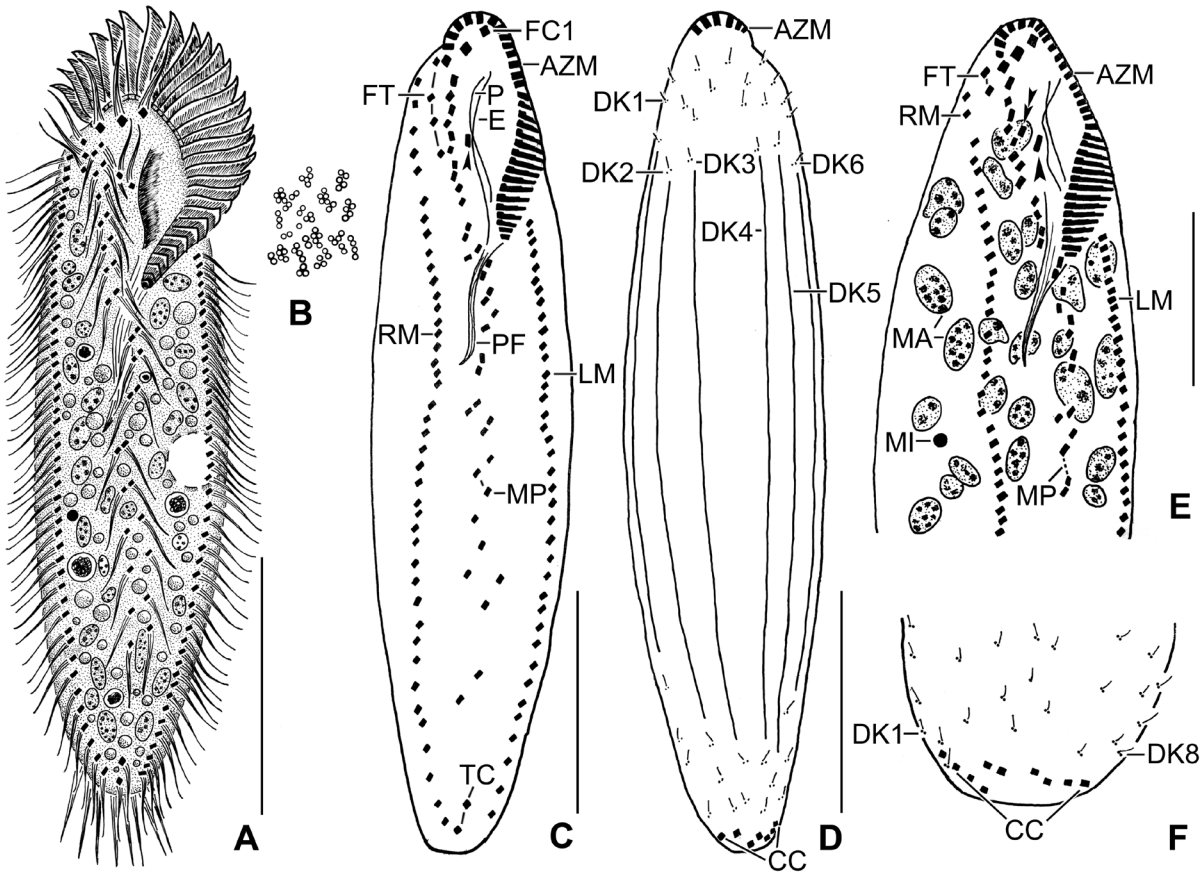

Fig. 6. *Neoholosticha vikali* gen. et sp. nov., line diagrams. **A–B**. Live specimens. **C–F**. Protargol-impregnated specimen. **A**. Ventral view of a representative specimen. **B**. Cortical granules arranged in small groups. **C–D**. Ventral (C) and dorsal (D) views of the holotype (NZSI) showing its infraciliature; arrowhead in C indicates the buccal cirrus. **E–F**. Ventral (E) and dorsal (F) views of paratype specimens (NZSI) depicting oral and somatic infraciliature as well as the nuclear apparatus; arrowhead in E indicates the buccal cirrus, double arrowheads in E indicate the parabuccal cirrus. Abbreviations: see Material and methods. Scale bars: A = 50 μm; C–D = 30 μm; E = 15 μm.

Description

Body size 105–155 × 30–50 μm in vivo, usually about 135 × 40 μm, based on in vivo measurements (n = 3) and morphometric data (Table 2), with about 20% addition for preparation shrinkage (Foissner *et al.* 2002; Kumar & Foissner 2016; Kumar *et al.* 2016). Length:width ratio 3.7:1 (Table 2). Outline narrowly elliptical to very narrowly elliptical; dorsoventrally flattened (Figs 5A–B, D–F, 6A, C–D). Nuclear apparatus consists of 70–108 ellipsoidal to elongate ellipsoidal macronuclear nodules scattered across body, each studded with nucleoli. Micronuclei globular, difficult to recognize both in vivo and in protargol preparations, with each cell containing about one or two micronuclei (Figs 5A–B, D–G, 6A, E). Cortex flexible, with cortical granules arranged in small groups, yellowish-green, about 0.5 μm across. Contractile vacuole located slightly below mid-body near left cell margin (Figs 5B–C, 6A–B). Cytoplasm densely packed with lipid droplets (Figs 5A–C, 6A). Movement moderately rapid, without peculiarities.

Cirral pattern of usual variability (Table 2). Frontal cirri slightly enlarged, about 12 μm long in vivo. Buccal cirrus positioned about 6.8 μm posterior to anterior end of paroral (Figs 5D, F–G, 6A, C, E); one parabuccal cirrus (observed in three out of 17 specimens analyzed). Two to four frontoterminal cirri, located posterior to distal end of adoral zone. Midventral complex composed of 15–18 cirral pairs only, extending to near transverse cirri. Pairs spaced slightly wider at posterior body end. Left and right marginal rows composed of equal numbers of cirri, except in one or two specimens with one to three additional cirri in right row (Figs 5D, F, 6A, C). Transverse cirri invariably (n = 9) two in number, ordinary-sized (about 10 μm long in vivo), and projecting beyond posterior body end (Figs 5A–B, D, F, 6A, C). Right marginal row with ~48 cirri, commencing at level of frontoterminal cirri and terminating near posterior body margin at level of transverse cirri (Figs 5D, F–G, 6A, C, E); left marginal row with ~45 cirri.

Dorsal ciliature consists of 6–8 dorsal kineties (Figs 5E, H, 6D, F), each bearing one or two caudal cirri. A total of 7–12 caudal cirri (Figs 5E, H, 6D, F).

Adoral zone of membranelles question mark-shaped, occupying on average 27% of body length in protargol preparations (Figs 5A–D, F–G, 6A, C, E; Table 2), with approximate DE-value of 0.2 (for explanation, see Berger 2006); composed of 26–38 membranelles, with largest bases about 5.1 μm wide in protargol preparations. Buccal field wide and deep. Paroral and endoral moderately curved and optically intersecting in middle (Figs 5D, F–G, 6A, C, E). Pharyngeal fibres extend slightly obliquely posteriorly (Figs 5C–D, F–G, 6A, C, E).

Occurrence and ecology

Thus far, the species has been found only at the type locality. It feeds on bacteria and small flagellates. Other ciliates identified from the same soil sample include *Monomacrocaryon* sp., *Sterkiella tricirrata* (Buitkamp, 1977) Berger 1999, and *Sterkiella tetracirrata* Kumar *et al.*, 2014. The soil from which the species was isolated contained 0.72% moisture, and has a pH of 6.69, an electrical conductivity of 445 μS, a Na^+ concentration of 30.5 mg/l, a K^+ concentration of 49.1 mg/l, 1.56% organic carbon, and 2.68% organic matter.

Discussion

Agricultural soil ciliate diversity

The present study contributes to the growing evidence that agricultural soils represent important reservoirs of ciliate diversity. Our findings add to the relatively few studies that have documented novel hypotrich taxa from arable fields (e.g., Foissner 1987; Bharti *et al.* 2017; Ghosh *et al.* 2024), underscoring the potential of agroecosystems to harbor unique and previously undescribed lineages. However, some reports have documented the community structure and population dynamics of ciliates from paddy fields

Table 2. Morphometric data on *Neoholisticha vikali* gen. et sp. nov.

Characteristic[a]	Mean	M	SD	SE	CV	Min	Max	n
body, length	114.0	114.0	11.2	2.4	9.8	87.0	130.0	21
body, width	31.0	31.0	4.2	0.9	13.5	23.0	40.0	21
body length:width, ratio	3.7	3.8	0.4	0.1	11.0	3.0	4.9	21
body width:length, percentage	27.2	26.5	3.0	0.6	10.9	20.5	33.0	21
anterior body end to proximal end of adoral zone, distance	30.6	31.0	1.8	0.4	6.0	26.0	34.0	21
anterior body end to distal end of adoral zone, distance	4.5	5.0	1.9	0.4	43.0	1.0	9.0	19
anterior body end to proximal end of adoral zone, % of body length	27.1	26.7	3.0	0.7	11.0	20.0	33.3	21
anterior body end to distal end of adoral zone, % of body length	3.9	4.0	1.8	0.4	44.4	0.9	8.2	19
DE-value (see text)	0.2	0.2	0.1	0.0	69.8	0.0	0.6	19
adoral membranelles, width of longest base	5.1	5.0	0.3	0.1	6.5	5.0	6.0	17
adoral membranelles, number	32.0	32.0	3.3	0.7	10.2	26.0	38.0	17
anterior body end to paroral membrane, distance	7.8	8.0	1.8	0.4	22.7	5.0	12.0	17
gap between adoral zone of membranelles and paroral membrane	6.8	7.0	1.9	0.5	27.4	3.0	10.0	16
paroral membrane, length	15.4	15.0	2.1	0.5	14.0	10.0	19.0	17
anterior body end to endoral, distance	8.1	8.0	1.5	0.4	18.4	5.0	11.0	17
endoral membrane, length	15.2	15.0	2.1	0.5	14.0	12.0	20.0	17
anteriormost macronuclear nodule, length	5.5	5.0	1.0	0.2	18.4	4.0	8.0	17
anteriormost macronuclear nodule, width	2.5	3.0	0.5	0.1	20.3	2.0	3.0	17
macronuclear nodules, number	84.7	85.0	10.2	2.5	12.1	70.0	108.0	17
micronucleus, length	1.5	1.0	0.5	0.1	35.5	1.0	2.0	13
micronucleus, width	1.2	1.0	0.4	0.1	32.5	1.0	2.0	13
micronucleus, number	1.5	1.0	0.5	0.1	35.5	1.0	2.0	13
anterior body end to right marginal row, distance	7.6	7.0	2.7	0.7	35.8	3.0	13.0	17
posterior body end to right marginal row, distance	3.0	3.0	1.5	0.4	50.2	1.0	7.0	16
right marginal row, number of cirri	48.0	47.0	5.3	1.3	11.0	40.0	61.0	16
anterior body end to left marginal row, distance	27.7	28.0	2.4	0.6	8.5	22.0	32.0	17
posterior body end to left marginal row, distance	1.6	1.0	1.1	0.3	66.0	1.0	4.0	15
left marginal row, number of cirri	44.8	45.0	6.2	1.6	13.9	37.0	57.0	15
frontal cirri, number	3.0	3.0	0.0	0.0	0.0	3.0	3.0	15
anterior body end to buccal cirrus, distance	14.2	14.0	2.6	0.7	18.7	9.0	18.0	13
buccal cirrus, number	1.0	1.0	0.0	0.0	0.0	1.0	1.0	15
parabuccal cirrus, number	1.0	1.0	0.0	0.0	0.0	1.0	1.0	3
frontoterminal cirri, number	2.6	2.0	0.8	0.2	29.4	2.0	4.0	14
midventral pairs, number	16.4	16.0	1.2	0.4	7.6	15.0	18.0	12
transverse cirri, number	2.0	2.0	0.0	0.0	0.0	2.0	2.0	9
dorsal kineties, number	6.9	7.0	0.9	0.3	12.7	6.0	8.0	10
caudal cirri, number	8.5	7.0	1.9	0.6	22.7	7.0	12.0	12

[a] Data based on mounted, protargol-impregnated, and randomly selected specimens from a non-flooded Petri dish culture. Measurements in µm. Abbreviations: CV = coefficient of variation in %; M = median; Max = maximum; Mean = arithmetic mean; Min = minimum; n = number of individuals investigated; SD = standard deviation; SE = standard error of arithmetic mean.

(e.g., Schwarz & Frenzel 2003; Murase *et al.* 2006; Martínez 2025). The detection of two new species belonging to two new genera from a single locality in Mathura, India, suggests that much of the soil ciliate diversity in India remains unexplored, particularly when compared with better-studied aquatic environments. Furthermore, the coexistence of ciliates with diverse microbial communities highlights their ecological importance as regulators of bacterial and flagellate populations, which in turn influence nutrient cycling and soil fertility. Integrating species-level taxonomy with ecological and agronomic

data will therefore be critical for revealing distributional patterns, adaptive strategies, and the potential functional roles of soil ciliates in sustaining agricultural productivity.

Comparison of *Pseudourosomoida* gen. nov. with similar genera

Among the six genera of the family Urosomoididae, the newly proposed genus *Pseudourosomoida* gen. nov. is mainly distinguished by the absence (vs presence) of caudal cirri. It differs from *Urosomoida* in morphogenesis, as primordia V and VI of the proter in *Pseudourosomoida* originate from the splitting of the opisthe's anlagen V and VI (vs possible de novo formation). It differs from *Erimophrya* by forming six frontal-ventral-transverse anlagen as usual (vs five in *Erimophrya*). The genus *Hemiurosomoida* can be separated from *Pseudourosomoida* by the presence of curved and non-intersecting (vs curved and optically intersecting) undulating membranes. *Lepidothrix* differs from *Pseudourosomoida* gen. nov. in having undulating membranes reaching the anterior left of the adoral zone of membranelles (vs distinctly posterior to the adoral zone). *Oxytrichella* is characterized by a single micronucleus between two macronuclear nodules (vs absence of micronuclei in *Pseudourosomoida*). *Paraurosomoida* can be distinguished by the absence (vs presence) of pretransverse and transverse cirri. For further details, see Berger (1999), Foissner *et al.* (2002), Singh & Kamra (2013), and Foissner (2016).

Comparison of *Pseudourosomoida kadamberiae* gen. et. sp. nov. with related species

On the basis of the number of micronuclei and the presence of pretransverse cirri, the new species can be compared with 14 species belonging to the family Urosomoididae, namely: *Erimophrya arenicola* Foissner *et al.*, 2002; *Hemiurosomoida koreana* Omar *et al.*, 2024; *Hemiurosomoida warreni* Chen *et al.*, 2021; *Lepidothrix dorsiincisura* (Foissner, 1982) Foissner 2016 (Galápagos population); *Lepidothrix reticulata* (Foissner *et al.*, 2002) Foissner 2016 (Costa Rica population); *Oxytrichella buitkampi* (Dragesco & Dragesco-Kernéis, 1986) Foissner 2016; *Oxytrichella mahadjacola* Foissner, 2016; *Oxytrichella monostyla* (Foissner *et al.*, 2002) Foissner 2016; *Oxytrichella perthensis* (Foissner & O'Donoghue, 1990) Foissner 2016; *Oxytrichella sejongensis* (Jung *et al.*, 2016) Li *et al.* 2017; *Urosomoida antarctica* Foissner, 1996; *Urosomoida galapagensis* Foissner & Libetreu in Foissner, 2016; *Urosomoida halophila* Foissner, 2016; and *Urosomoida namibiensis* Foissner *et al.*, 2002.

Erimophrya arenicola can be distinguished from *Pseudourosomoida kadamberiae* gen.et sp. nov. by the absence (vs presence) of cortical granules, the presence of one to three (vs absence) micronuclei, fewer adoral membranelles (13–17 vs 17–30), a single (vs invariably three) postoral ventral cirrus, the absence (vs invariably one) of pretransverse cirri, a single (vs invariably four) transverse cirrus, and three (vs invariably four) dorsal kineties.

Hemiurosomoida koreana differs from *Pseudourosomoida kadamberiae* gen. et sp. nov. in having one or two (vs absent) micronuclei, four or five (vs invariably four) frontoventral cirri, two (vs invariably one) pretransverse ventral cirri, four or five (vs invariably four) transverse cirri, and two (vs absent) caudal cirri. Additionally, in *H. koreana*, the dorsomarginal kinety ends in the anterior third of the body (vs extending almost to the posterior end, only slightly shortened posteriorly). *Hemiurosomoida warreni* can be separated from *Pseudourosomoida kadamberiae* by its larger body size (85–138 μm × 22–42 μm vs 45–67 μm × 15–25 μm in protargol preparations), the presence of four to eight globular to ellipsoidal moniliform macronuclear nodules (vs invariably two ellipsoidal nodules), and higher numbers of cirri in the right and left marginal rows (29–39 and 26–35 vs 12–21 and 14–20, respectively).

The Costa Rican population *of Lepidothrix reticulata* can be distinguished from *Pseudourosomoida kadamberiae* gen. et sp. nov. by its larger body size (106–142 μm × 22–46 μm vs 45–67 μm × 15–25 μm); the presence of a cortex with a web-like pattern formed by numerous bright globules arranged in single, paired, or occasionally triplet short rows (vs colorless to yellowish cortical granules); one to four (vs absent) micronuclei; a slightly higher number of adoral membranelles (25–42 vs 17–30); right

and left marginal cirri (31–46 and 23–42 vs 12–21 and 14–20, respectively); pretransverse ventral cirri (three or four vs invariably one); and two or three (vs invariably four) transverse cirri. Similarly, the Galápagos population of *Lepidothrix dorsiincisura* differs from *Pseudourosomoida kadamberiae* by its larger body size (86–123 μm × 28–50 μm vs 45–67 μm × 15–25 μm); the presence of four (vs invariably two) macronuclear nodules; a slightly higher number of adoral membranelles (27–42 vs 17–30); right and left marginal cirri (22–31 and 20–29 vs 12–21 and 14–20, respectively); a total of three or four (vs invariably five) pretransverse and transverse cirri; and the presence (vs absence) of caudal cirri.

Oxytrichella buitkampi can be separated from *Pseudourosomoida kadamberiae* gen. et sp. nov. by the absence (vs presence) of cortical granules, the presence of a single micronucleus (vs absence of micronuclei), five (vs invariably four) transverse cirri, and three or four (vs absent) caudal cirri. *Oxytrichella mahadjacola* differs from the new species by the absence (vs presence) of cortical granules, the presence of one micronucleus (vs absence of micronuclei), and fewer right and left marginal cirri (3–5 and 5–7 vs 12–21 and 14–20, respectively). *Oxytrichella monostyla* is distinguishable from *Pseudourosomoida kadamberiae* by the absence (vs presence) of cortical granules, the presence of a single micronucleus (vs absence of micronuclei), fewer adoral membranelles (13–15 vs 17–30), a single (vs invariably three) postoral ventral cirrus, and its occurrence in a highly saline (vs terrestrial) habitat. *Oxytrichella perthensis* differs from the new species by the absence (vs presence) of cortical granules, one micronucleus (vs absence of micronuclei), three or four (vs invariably three) postoral ventral cirri, two (vs invariably one) pretransverse ventral cirri, and three (vs four) transverse cirri. *Oxytrichella sejongensis* can be differentiated from *Pseudourosomoida kadamberiae* by its larger body size (71.5–110.5 μm × 22.6–38.1 μm vs 45–67 μm × 15–25 μm), the presence of a single micronucleus (vs absence of micronuclei), higher numbers of right and left marginal cirri (28–33 and 26–32 vs 12–21 and 14–20, respectively), and occurrence in freshwater (vs terrestrial) habitat.

Urosomoida antarctica differs from *Pseudourosomoida kadamberiae* gen. et sp. nov. by the absence (vs presence) of cortical granules, the presence of one to three micronuclei (vs absence of micronuclei), fewer postoral ventral cirri (one vs three), pretransverse ventral cirri (two vs one), transverse cirri (five or six vs four), and the presence (vs absence) of caudal cirri. *Urosomoida galapagensis* can be distinguished from the new species by its slightly larger body size (70–89 × 22–40 μm vs 45–67 × 15–25 μm), presence (vs absence) of micronuclei, slightly higher numbers of cirri in the right and left marginal rows (20–28 and 19–27 vs 12–21 and 14–20, respectively), one to three (vs invariably one) pretransverse cirri, presence (vs absence) of caudal cirri, and its occurrence in a highly saline habitat (vs terrestrial). *Urosomoida halophila* differs from *Pseudourosomoida kadamberiae* by the absence (vs presence) of cortical granules, presence (vs absence) of micronuclei, a shorter adoral zone (occupying 16–27% vs 27.6–43.3% of the body length), more pretransverse ventral cirri (two or three vs always one), presence (vs absence) of caudal cirri, and saline (vs terrestrial) habitat. *Urosomoida namibiensis* can be separated from the new species by its larger body size (91–133 × 25–44 μm vs 45–67 × 15–25 μm), four (vs invariably two) macronuclear nodules, a slightly shorter adoral zone (occupying 19–30% vs 27.6–43.3% of the body length), two to five (vs invariably five) pretransverse ventral and transverse cirri, and the presence (vs absence) of caudal cirri. For further details, see Berger (1999), Foissner *et al.* (2002), Foissner (2016), Jung *et al.* (2016), Li *et al.* (2017), Omar *et al.* (2024), and Singh & Kamra (2013).

Comparison of *Neoholosticha* gen. nov. with similar genera

Among the 13 genera of the family Holostichidae, *Neoholosticha* gen. nov. is mainly distinguished by the presence of 6–8 dorsal kineties and 7–12 caudal cirri (Berger 2006; Li *et al.* 2017).

The genus *Acuholosticha* differs from *Neoholosticha* gen. nov. by having a narrowly rounded (vs flattened) posterior end, pretransverse ventral cirri present or absent (vs absent), and two to four (vs six to eight) dorsal kineties. *Adumbratosticha* is distinguished by an elongate rectangular body with

a rounded posterior end (vs ellipsoidal with a flattened posterior end), fewer caudal cirri (often two) than dorsal kineties, and in some species vestigial caudal cirri (vs always more caudal cirri than dorsal kineties). It also has relatively short, almost straight, non-intersecting (vs long and optically intersecting) undulating membranes, and pretransverse ventral cirri present or absent (vs absent). *Afrothrix* differs by possessing a bipartite (vs continuous) adoral zone of membranelles and the absence (vs presence) of caudal cirri. *Anteholosticha* can be separated by having transverse cirri usually fewer than midventral pairs (vs invariably two) and by the absence (vs presence) of caudal cirri. *Caudikeronopsis* differs by the presence (vs absence) of pretransverse ventral cirri and occurrence in marine (vs terrestrial) habitats. *Diaxonella* is distinguished by having two or more (vs a single) left marginal rows. *Extraholosticha* differs by the presence (vs absence) of a short cirral row between the left frontal cirrus and the undulating membranes. *Holosticha* differs, inter alia, by having a gap between the proximal and distal parts of the adoral zone of membranelles (vs continuous adoral zone), short and parallel (vs long and optically intersecting) undulating membranes, transverse cirri equal to or slightly fewer than midventral pairs (vs invariably two), and the absence (vs presence) of caudal cirri. *Limnoholosticha* is distinguished by an elliptical to wide elliptical body (vs slender elliptical), five to eight (vs invariably two) transverse cirri, and occurrence in stagnant inland waters (vs terrestrial habitats). *Multiholosticha* differs by the presence (vs absence) of pretransverse ventral cirri, seven to twelve (vs invariably two) transverse cirri, and a freshwater (vs terrestrial) habitat. *Periholosticha* can be separated by having a bipartite (vs continuous) adoral zone, the buccal cirrus absent (vs present), and midventral pairs that extend only shortly (vs extending almost to the transverse cirri). *Psammomitra* differs by its tripartite (vs ellipsoidal) body form, short and parallel (vs long and intersecting) undulating membranes, and the absence (vs presence) of caudal cirri. *Pseudoamphisiella* is distinguished by the absence (vs presence) of frontoterminal cirri and by having multiple (vs invariably two) transverse cirri.

Comparison of *Neoholosticha vikali* gen. et. sp. nov. with related species

Based on the body shape, multiple macronuclear nodules, the presence of a continuous adoral zone of membranelles, single left and right marginal cirral rows, more than three dorsal kineties, more than three caudal cirri, and the absence of a cirral row between the left frontal cirrus and the undulating membranes, *Neoholosticha vikali* gen. et sp. nov. can be compared with two species of the family *Holostichidae*, viz., *Multiholosticha multicaudicirrus* (Song & Wilbert, 1989) Li *et al.* 2017 and *Multiholosticha interrupta* (Dragesco, 1966) Li *et al.* 2017.

Multiholosticha multicaudicirrus can be separated from the new species by having slightly smaller body size (61–95 μm × 27–45 μm vs 87–130 μm × 23–40 μm), fewer macronuclear nodules (29–32 vs 70–108), a slightly longer adoral zone (occupying ~39% vs ~27% of the body length), a higher number of frontal cirri (four or five vs invariably three), fewer midventral pairs (five to eight vs 15–18), seven to ten (vs only two) transverse cirri, fewer cirri in the right and left marginal rows (22–27 and 20–26 vs 40–61 and 37–57, respectively), slightly fewer dorsal kineties (six or seven vs six to eight), and five to seven (vs seven to twelve) caudal cirri.

Multiholosticha interrupta differs from *Neoholosticha vikali* gen. et sp. nov. by a longer body (~200 μm vs ~114 μm), ~30 (vs ~85) macronuclear nodules, a slightly longer adoral zone (occupying ~36% vs ~27% of the body length), a slightly smaller number of midventral pairs (~9–11 vs ~15–18), the presence (vs absence) of pretransverse ventral cirri, 11 or 12 (vs only two) transverse cirri, a slightly lower number of right marginal cirri (30–40 vs 40–61), and six (vs six to eight) dorsal kineties. For further details, see Berger (2006) and Li *et al.* (2017).

Conclusion

This study provides detailed taxonomic descriptions of two novel hypotrich ciliates, *Pseudourosomoida kadamberiae* gen. et sp. nov. and *Neoholosticha vikali* gen. et sp. nov., thereby advancing our

understanding of soil ciliate diversity and taxonomy. The comprehensive morphological and ontogenetic analyses presented here establish a solid taxonomic framework that is indispensable for future research on soil protist biodiversity. Although detailed ecological and agronomic data from the sampling site were not available, the discovery of these previously undescribed taxa highlights agricultural soils as important reservoirs of hidden microbial eukaryotic diversity. Moving forward, integrative approaches that combine morphology, molecular analyses, soil ecological parameters, and agronomic management practices will be crucial for elucidating the functional roles of ciliates in agroecosystems and their contributions to soil biodiversity and health.

Acknowledgments

The authors gratefully thank Dr Dhriti Banerjee, Director of the Zoological Survey of India, Kolkata, India, for her support throughout all stages of the present research and for providing the necessary facilities to carry out the research work. CSIR-India fellowship to Mr Arnab Ghosh is also duly acknowledged. The authors sincerely thank the Section editor, Dr Peter Vďačný, and the anonymous reviewers for their constructive comments and suggestions, which greatly improved the manuscript.

References

Ammermann D., Steinbruck G., von Berger L. & Hennig W. 1974. The development of the macronucleus in the ciliated protozoan *Stylonychia mytilus*. *Chromosoma* 45: 401–429. https://doi.org/10.1007/BF00283386

Anthony M.A., Bender S.F. & van der Heijden M.G.A. 2023. Enumerating soil biodiversity. *Proceedings of the National Academy of Sciences of the United States of America* 120 (33): e2304663120. https://doi.org/10.1073/pnas.2304663120

Berger H. 1999. Monograph of Oxytrichidae (Ciliophora, Hypotrichia). *Monographiae Biologicae* 78: 1–1080. https://doi.org/10.1007/978-94-011-4637-1

Berger H. 2003. Redefinition of *Holosticha* Wrzesniowski, 1877 (Ciliophora, Hypotricha). *European Journal of Protistology* 39: 373–379.

Berger H. 2006. Monograph of the Urostyloidea (Ciliophora, Hypotrichia). *Monographiae Biologicae* 85: 1–1304. https://doi.org/10.1007/1-4020-5273-1

Bharti D., Kumar S. & La Terza A. 2015. Two gonostomatid ciliates from the soil of Lombardia, Italy; including note on the soil mapping project. *Journal of Eukaryotic Microbiology* 62: 762–772. https://doi.org/10.1111/jeu.12234

Bharti D., Kumar S., Basuri C.K. & La Terza A. 2024. Ciliated protist communities in soil: contrasting patterns in natural sites and arable lands across Italy. *Soil Systems* 8: 64. https://doi.org/10.3390/soilsystems8020064

Chaurasia S. & Gupta A.D. 2014. *Handbook of Water, Air, and Soil Analysis (A Lab Manual)*. International E-Publication, India.

Fauré-Fremiet E. 1961. Remarques sur la morphologie comparée et la systématique des Ciliata Hypotrichida. *Comptes rendus hebdomadaires des Séances de l'Académie des Sciences* 252: 3515–3519.

Foissner W. 1982. Ökologie und Taxonomie der Hypotrichida (Protozoa: Ciliophora) einiger österreichischer Böden. *Archiv für Protistenkunde* 126: 19–143. https://doi.org/10.1016/S0003-9365(82)80065-1

Foissner W. 1987. The micro-edaphon in ecofarmed and conventionally farmed dryland cornfields near Vienna (Austria). *Biology and Fertility of Soils* 3 (1): 45–49.

Foissner W. 1991. Basic light and scanning electron microscopic methods for taxonomic studies of ciliated protozoa. *European Journal of Protistology* 27: 313–330. https://doi.org/10.1016/S0932-4739(11)80248-8

Foissner W. 1992. Comparative studies on the soil life in ecofarmed and conventionally farmed fields and grasslands of Austria. *Agriculture, Ecosystems & Environment* 40 (1–4): 207–218. https://doi.org/10.1016/0167-8809(92)90093-Q

Foissner W. 2016. Terrestrial and semiterrestrial ciliates (Protozoa, Ciliophora) from Venezuela and Galapágos. *Denisia* 35: 1–912.

Foissner W., Agatha S. & Berger H. 2002. Soil ciliates (Protozoa, Ciliophora) from Namibia (Southwest Africa), with emphasis on two contrasting environments, the Etosha region and the Namib Desert. *Denisia* 5: 1–1459.

Geisen S., Mitchell E.A.D., Wilkinson D.M., Adl S., Bonkowski M., Brown M.W., Fiore-Donno A.M., Heger T.J., Jassey V.E., Krashevska V., Lahr D.J.G., Marcisz K., Mulot M., Payne R., Singer D., Anderson O.R., Charman D.J., Ekelund F., Griffiths B.S., Rønn R., … & Lara E. 2017. Soil protistology rebooted: 30 fundamental questions to start with. *Soil Biology and Biochemistry* 111: 94–103. https://doi.org/10.1016/j.soilbio.2017.04.001

Ghosh A., Bharti D., Pathania P.C. & Kumar S. 2024. Description of two ciliated protists from agricultural soils of India. *Records of the Zoological Survey of India* 124: 1–10. https://doi.org/10.26515/rzsi/v124/i1/2024/169070

Ghosh A., Bharti D., Bhutiani R., Pathania P.C. & Kumar S. 2025. Morphology, morphogenesis, and molecular phylogeny of an Indian population of *Notohymena quadrinucleata* Foissner, 2016 (Ciliophora: Oxytrichidae). *Journal of Natural History* 59: 1917–1931. https://doi.org/10.1080/00222933.2025.2498720

Hemberger H. 1985. Neue Gattungen und Arten hypotricher Ciliaten. *Archiv für Protistenkunde* 130 (4): 397–417. https://doi.org/10.1016/S0003-9365(85)80051-8

Jung J.H., Baek Y.S., Kim S. & Choi H.G. 2016. Morphology and molecular phylogeny of a new freshwater ciliate *Urosomoida sejongensis* n. sp. (Ciliophora, Sporadotrichida, Oxytrichidae) from King George Island, Antarctica. *Zootaxa* 4072: 254–262. https://doi.org/10.11646/zootaxa.4072.2.7

Kamra K. & Sapra G.R. 1990. Partial retention of parental ciliature during morphogenesis of the ciliate *Coniculostomum monilata* (Dragesco and Njiné, 1971) Njiné, 1978 (Oxytrichidae, Hypotrichida). *European Journal of Protistology* 25: 264–278. https://doi.org/10.1016/S0932-4739(11)80179-3

Kumar S. & Foissner W. 2016. High cryptic soil ciliate (Ciliophora, Hypotrichida) diversity in Australia. *European Journal of Protistology* 53: 61–95. https://doi.org/10.1016/j.ejop.2015.10.001

Kumar S., Bharti D., Quintela-Alonso P., Shin M.K. & La Terza A. 2016. Fine-tune investigations on three stylonychid (Ciliophora, Hypotricha) ciliates. *European Journal of Protistology* 56: 200–218. https://doi.org/10.1016/j.ejop.2016.09.006

Li F., Lyu Z., Li Y., Fan X., Al-Farraj S.A., Shao C. & Berger H. 2017. Morphology, morphogenesis, and molecular phylogeny of *Uroleptus* (*Caudiholosticha*) *stueberi* (Foissner, 1987) comb. nov. (Ciliophora, Hypotricha), and reclassification of the remaining *Caudiholosticha* species. *European Journal of Protistology* 59: 82–98. https://doi.org/10.1016/j.ejop.2016.08.007

Martínez S. 2025. Protist community structure and functional diversity in soils of rice rotations with crops and pastures. *Applied Soil Ecology* 213: 106310. https://doi.org/10.1016/j.apsoil.2025.106310

Murase J., Noll M. & Frenzel P. 2006. Impact of protists on the activity and structure of the bacterial community in a rice field soil. *Applied and Environmental Microbiology* 72: 5436–5444. https://doi.org/10.1128/AEM.00207-06

Omar A., Moon J.H. & Jung J.H. 2024. Morphology and molecular phylogeny of two hypotrichous ciliates (Ciliophora, Spirotrichea) from South Korea, including *Hemiurosomoida koreana* n. sp. *European Journal of Protistology* 92: 126045. https://doi.org/10.1016/j.ejop.2023.126045

Schwarz M.J. & Frenzel P. 2003. Population dynamics and ecology of ciliates (Protozoa, Ciliophora) in an anoxic rice field soil. *Biology and Fertility of Soils* 38: 245–252. https://doi.org/10.1007/s00374-003-0644-z

Shao C., Song W., Al-Rasheid K.A. & Berger, H. 2012. Redefinition and reassignment of the 18-cirri genera *Hemigastrostyla*, *Oxytricha*, *Urosomoida*, and *Actinotricha* (Ciliophora, Hypotricha), and description of one new genus and two new species. *Acta Protozoologica* 50: 263–287. https://doi.org/10.4467/16890027AP.11.025.0062

Singh J. & Kamra K. 2013. *Paraurosomoida indiensis* gen. nov., sp. nov., an oxytrichid (Ciliophora, Hypotricha) from Kyongnosla Alpine Sanctuary, including note on non-oxytrichid Dorsomarginalia. *European Journal of Protistology* 49: 600–610. https://doi.org/10.1016/j.ejop.2013.04.001

Singh J. & Kamra K. 2015. Molecular phylogeny of *Urosomoida agilis*, and new combinations: *Hemiurosomoida longa* gen. nov., comb. nov., and *Heterourosomoida lanceolate* gen. nov., comb. nov. (Ciliophora, Hypotricha). *European Journal of Protistology* 51: 55–65. https://doi.org/10.1016/j.ejop.2014.11.005

Song W., Zhang T., Zhang X., Warren A., Song W., Zhao Y. & Luo X. 2021. Taxonomy, ontogenesis and evolutionary relationships of the algae-bearing ciliate *Bourlandella viridis* comb. nov., with establishment of a new genus and new family (Protista, Ciliophora, Hypotrichia). *Frontiers in Microbiology* 11: 560915. https://doi.org/10.3389/fmicb.2020.560915

Wallengren H. 1900. Zur Kenntnis der vergleichenden Morphologie der hypotrichen Infusorien. *Bihang till Kongliga Svenska vetenskaps-akademiens handlingar* 26: 1–31.

Warren A., Patterson D.J., Dunthorn M., Clamp J.C., Achilles-Day U.E., Aescht E., Al-Farraj S.A., Al-Quraishy S.A., Al-Rasheid K.A.S., Carr M., Day J.G., Dellinger M., El-Serehy H.A., Fan Y., Gao F., Gao S., Gong J., Gupta R., Hu X., … & Agatha S. 2017. Beyond the "Code": A guide to the description and documentation of biodiversity in ciliated protists (Alveolata, Ciliophora). *Journal of Eukaryotic Microbiology* 64: 539–554. https://doi.org/10.1111/jeu.12391

Printed versions of all papers are deposited in the libraries of two of the institutes that are members of the *EJT* consortium: Muséum national d'Histoire naturelle, Paris, France and Royal Museum for Central Africa, Tervuren, Belgium. The other members of the consortium are: Royal Belgian Institute of Natural Sciences, Brussels, Belgium; Meise Botanic Garden, Meise, Belgium; Natural History Museum of Denmark, Copenhagen, Denmark; Naturalis Biodiversity Center, Leiden, the Netherlands; Museo Nacional de Ciencias Naturales-CSIC, Madrid, Spain; Leibniz Institute for the Analysis of Biodiversity Change, Bonn – Hamburg, Germany; National Museum of the Czech Republic, Prague, Czech Republic; The Steinhardt Museum of Natural History, Tel Aviv, Israël.